The Journal of Experimental Biology 204, 2597–2605 (2001)
Printed in Great Britain © The Company of Biologists Limited 2001
JEB3339

REVIEW

STRUCTURE–FUNCTION RELATIONSHIPS OF A-, F- AND V-ATPases

GERHARD GRÜBER[1,*], HELMUT WIECZOREK[2], WILLIAM R. HARVEY[3] AND VOLKER MÜLLER[4]

[1]*FR 2.5 Biophysik, Universität des Saarlandes, D-66421 Homburg, Germany,* [2]*Department of Biology, University of Osnabrück, D-49069 Osnabrück, Germany,* [3]*Whitney Laboratory, University of Florida, St Augustine, FL 32080, USA* and [4]*Lehrstuhl für Mikrobiologie der Ludwig-Maximilians-Universität München, D-80638, München, Germany*

*Author for correspondence (e-mail: ggrueber@ med-rz.uni-saarland.de)

Accepted 9 May 2001

Summary

Ion-translocating ATPases, such as the F_1F_o-, V_1V_o- and archaeal A_1A_o enzymes, are essential cellular energy converters which transduce the chemical energy of ATP hydrolysis into transmembrane ionic electrochemical potential differences. Based on subunit composition and primary structures of the subunits, these types of ATPases are related through evolution; however, they differ with respect to function. Recent work has focused on the three-dimensional structural relationships of the major, nucleotide-binding subunits A and B of the A_1/V_1-ATPases and the corresponding β and α subunits of the F_1-ATPase, and the location of the coupling subunits within the stalk that provide the physical linkage between the regions of ATP hydrolysis and ion transduction. This review focuses on the structural homologies and diversities of A_1-, F_1- and V_1-ATPases, in particular on significant differences between the stalk regions of these families of enzymes.

Key words: A_1A_o-ATPase, archaea-type ATPase, F_1F_o-ATPase, H^+ translocating vacuolar-type ATPase, V_1-ATPase, small-angle X-ray scattering, *Escherichia coli*, *Manduca sexta*, *Methanosarcina mazei*.

Introduction

Adenosine 5′-triphosphate (ATP) synthesis by oxidative phosphorylation or photophosphorylation is a multi-step, membrane-located process that provides the bulk of cellular energy in eukaryotes and many prokaryotes. Most of the ATP synthesis in these cells is catalyzed by the enzyme, F_1F_o-ATP synthase, also called F_1F_o-ATPase (F-ATPase), which in its simplest, bacterial, form is composed of eight subunits (α_3:β_3:γ:δ:ε:*a*:b_2:$c_{9–12}$). The archaeal A_1A_o-ATP synthase (A-ATPase) has ten subunits (A_3:B_3:C:D:E:F:G:H:I:K_x), the actual subunit stoichiometry being unknown. The term ATPase reflects the fact that the F- and A-enzymes are reversible and can act as proton (or Na^+)-pumping complexes. The F- and the A-ATPases transform energy from a gradient of ions across the membrane to synthesize ATP (Mitchell, 1961; Dimroth, 1997; Müller et al., 1999). Conversely, the free energy of ATP hydrolysis can be coupled to proton (or Na^+) translocation and generate an ion-motive force (*IMF*), as in the genetically related vacuolar-type, H^+-translocating ATPases (V-ATPases). The V-ATPases, consisting of at least twelve distinct subunits (A_3:B_3:C:D:E:F:G_y:H_z:a:d:e:c_6), generate *IMFs* that are used for ligand trafficking, signaling, nutrient uptake and diverse activities in endomembranes and plasma membranes of animal cells (Wieczorek et al., 1999).

A-, V- and F-ATPases consist of a mosaic of globular structural units, including domain and secondary structures, which also serve as functional units. Morphologically each of these enzymes has three components: a membrane-bound sector, $A_o/F_o/V_o$, which contains the ion channel, a central connecting stalk, and an approximately spherical assembly, $A_1/F_1/V_1$, which contains the catalytic sites (Schäfer et al., 1999; Leslie and Walker, 2000; Forgac, 2000). Side-view projections of the F_1F_o- (Wilkens and Capaldi, 1998) and V_1V_o-ATPases (Boekema et al., 1997) show a *second* stalk (stator) as a fourth distinct feature extending from the F_o or V_o portion. In the case of the *Escherichia coli* F_1 moiety the central stalk is composed of γ_{ec} and ε_{ec}, which are the equivalent of δ_m in mitochondrial F_1F_o, and the stator is formed by the δ_{ec} and b subunits (Pedersen et al., 2000). The bacterial δ subunit (δ_{ec}) bears homology to one of the mitochondrial F_o subunits called OSCP (Table 1). The mitochondrial F_1 ε subunit (ε_m) has no counterpart in the bacterial F_1F_o enzyme. The central element of the F_1 complex, subunit γ, has been shown to move relative to the $\alpha_3\beta_3$ complex during ATP hydrolysis (Capaldi et al., 1996; Junge et al., 1997; Masaike et al., 2000). This rearrangement is proposed to drive the motion of a ring of $c_{9–14}$ subunits (Fillingame, 1996; Stock et al., 1999; Seelert et al., 2000; Stahlberg et al., 2001) in the F_o domain (Sambongi et al., 1999; Pänke et al., 2000; Tsunoda et al.,

Table 1. *Listing of similar ATPase gene products in the A-, F- and V-ATPases*

M. mazei Gö1 A_1A_O	*M. sexta* V_1V_O	*Bovine* F_1F_O	*E. coli* F_1F_O
A	A	β	β
B	B	α	α
C	C	–	–
–	D	–	–
D	E	γ	γ
E	–	OSCP	δ_{ec}
F	F	δ_m	ε_{ec}
–	G	–	–
–	H	–	–
–	–	ε_m	–
I	*a*	*a+b*	*a+b*
K	*c*	*c*	*c*
-	*d*	–	–
–	*e*	–	–
H	–	–	–
G	–	–	–
–	–	*d*	–
–	–	*e*	–
–	–	*f*	–
–	–	*g*	–
–	–	F_6	–
–	–	IF_1	–

2001), each containing two transmembrane helices (Rastogi and Girvin, 1999).

Based on their subunit composition and primary sequences, the A-type (archaeal) enzymes are more closely related through evolution to V-type than to F-type ATPases (Iwabe et al., 1989; Ihara et al., 1992; Müller et al., 1999). Three interdigitating copies of the nucleotide-binding subunits A and B of the A_1/V_1-ATPases and subunits β and α of the F_1-ATPase, respectively, exhibit more than 25 % primary sequence identity (Nelson, 1992). The minor subunits C, D, E, F, G and C, D, E, F, G, H of the A_1 and V_1-ATPases, respectively, form the stalk and are proposed, by analogy to F-ATPases, to be involved, either directly or indirectly, in conversion of energy into controlled motion (Müller et al., 1999; Grüber et al., 2000a). However, the minor stalk subunits of A_1, F_1 and V_1-ATPases show much less similarity than the headpiece subunits, suggesting that there are differences between the three classes of enzyme (Müller et al., 1999). One fundamental distinction is the reversible dissociation of the V_1 from the V_o complex as an *in vivo* regulatory mechanism for the control of V-ATPase activity (Wieczorek et al., 2000). By contrast, the A_1/F_1 and A_o/F_o sectors form stable associated complexes in the cell. Moreover, A- and F-ATPases, unlike V-ATPases, share the ability to synthesize ATP. Nevertheless, lineage profiles based on primary sequence reveal that A- and V-ATPases are more closely related to each other than to F-ATPases (Schäfer et al., 1999). Despite the fact that A-ATPases display chimeric properties of V- and F-ATPases the structure/function relationships of these enzymes remain a mystery. This review will focus on recent advances in elucidating structural and functional relationships of A_1/V_1- and F_1-ATPases.

F_1-ATPase: structure and subunit function

Structure description of the F_1 headpiece

Over the past decade, a tremendous amount of structural information about the F_1F_o-ATPase has been obtained using electron microscopy (reviewed in Gogol, 1994; Böttcher and Gräber, 2000), macromolecular crystallography (Abrahams et al., 1994; Shirakihara et al., 1997; Bianchet et al., 1998; Hausrath et al., 1999; Stock et al., 1999; Groth and Pohl, 2001) and nuclear magnetic resonance (NMR) spectroscopy (Wilkens et al., 1995; Wilkens et al., 1997; Rastogi and Girvin, 2000). Significant insights into the molecular mechanism of ATP hydrolysis came from the X-ray structure of the bovine heart $\alpha_3\beta_3\gamma$ complex of the F_1-ATPase (MF_1; Abrahams et al., 1994). The crystallographic model describes the three alternating α and β subunits as being arranged hexagonally, surrounding a solvent-filled cavity which is traversed by a part of the γ subunit. This coiled-coil structure of the γ subunit is asymmetrically located in the shaft relative to the axis of the $\alpha_3\beta_3$ complex and protrudes from it by about 30 Å into the stalk region. A third short α-helix of the γ subunit is inclined at a 45 ° angle to the coiled-coil domain at the bottom of the F_1 as it merges with the stalk that connects the F_1 and F_o parts. A key feature of the structural model is its asymmetry, particularly in the nucleotide occupancy and conformations of the catalytic β subunits. One β subunit, designated β_{TP}, is ligated with MgAMP-PNP and linked to the short α-helix of the γ subunit via the C-terminal domain. A second β subunit, β_{DP}, has MgADP bound and the third catalytic site, β_E, is free of nucleotides and Mg^{2+}. The three non-catalytic α subunits are ligated with MgAMP·PNP and adopt similar conformations, although one α subunit, which contributes to β_{TP} and is therefore denoted α_{TP}, displays a small rigid body rotation of the top domain relative to the other two domains (Abrahams et al., 1994).

Arrangement of the stalk subunits

Neither the structural model of the bovine F_1-ATPase (Abrahams et al., 1994) nor the subsequently determined structure of rat liver F_1-ATPase (Bianchet et al., 1998), which includes almost all of the residues of the α and β subunits, include either the small subunits δ_m and ε_m, or approximately half of the γ subunit residues. Subsequently, crystals containing all five subunits of the *Escherichia coli* F_1-ATPase ($\alpha_3:\beta_3:\gamma:\delta_{ec}:\varepsilon_{ec}$) and the $\alpha_3\beta_3\gamma\varepsilon_{ec}$ complex of the same organism have been obtained and diffracted to a resolution of 6.4 Å and 4.4 Å, respectively (Grüber et al., 1997; Hausrath et al., 1999). Besides the α and β subunits and the known part of the coiled-coil α-helices of the MF_1 the electron-density map at 4.4 Å extends 12 and 20 residues, respectively, thereby adding 15 Å to the length of the N-terminal α-helix and 23 Å to the C-terminal helix of the γ subunit (Hausrath et al., 1999). This structure reveals that γ extends from the $\alpha_3\beta_3$ hexagon far

enough to traverse the full length of the central stalk, in agreement with the refined crystal structure at 2.4 Å resolution of the γ_{ec}-ε_{ec} complex from *E. coli* (Rodgers and Wilce, 2000) and the complete bovine F_1-ATPase (Fig. 1; Gibbons et al., 2000). In these structural models the γ subunit is arranged in six α-helices and five β-stranded β-sheets (Rodgers and Wilce, 2000; Gibbons et al., 2000). The bottom of γ is in contact with the external loops of *c* subunits (Watts et al., 1995; Watts et al., 1996); the entire γ subunit makes up a coupling domain, which couples ATP hydrolysis with ion pumping (Capaldi et al., 1996; Junge et al., 1997). Adjacent to the 'bottom' part of subunit γ an additional density has been observed in the map obtained from crystals of the $\alpha_3\beta_3\gamma\delta\varepsilon c_{10}$ subcomplex of yeast mitochondrial ATP synthase at a 3.9 Å resolution (Stock et al., 1999) and the bovine F_1 (Gibbons et al., 2000). In these densities the structure of the ε_{ec} subunit (Wilkens et al., 1995; Uhlin et al., 1997), the counterpart of the yeast (δ_{ye}; Giraud and Velours, 1994) and bovine δ subunit (Fig. 1; δ_m), has been modeled. Like subunit ε_{ec}, the subunits δ_{ye} and δ_m are composed of a C-terminal helix–loop–helix structure and an N-terminal 10-stranded β-sandwich structure. However, the modeling of the ε_{ec} subunit indicates that the C terminus of the polypeptide is turned away from the bottom domain of the catalytic β subunit. This domain is believed to be involved in the coupling of catalytic-site events (Capaldi et al., 1996; Grüber and Capaldi, 1996) along with γ and ε_{ec} acting as a rotor (reviewed in Junge et al., 1997; Masaike et al., 2000; Tsunoda et al., 2001). This structural feature is in conflict with the model of the γ_{ec}-ε_{ec} subcomplex (Rodgers and Wilce, 2000), in which the ε_{ec} is located in close proximity to β via its C-terminal α-helix and with its β-sandwich barrel turned toward the bottom of γ. As shown by cryo-electron microscopy (Gogol, 1994) and biochemical studies (Mendel-Hartwig and Capaldi, 1991; Wilkens and Capaldi, 1998), the ε_{ec} subunit can exist in different states in the complex depending upon whether ATP, MgATP or MgADP is bound to the enzyme (Mendel-Hartwig and Capaldi, 1991; Wilkens and Capaldi, 1998). Using *E. coli* F_1 mutants with cysteine substitutions in the C termini of the α, β and ε_{ec} subunits it has been shown that in the ATP-conformation, when the γ and ε_{ec} subunits are linked to α subunits, the high-affinity site is completely closed with nucleotide unable to get in or out. In contrast, in the ADP-conformation, when the small subunits are linked to β subunits, there is nucleotide exchange in and out from the high catalytic site (Grüber and Capaldi, 1996). Therefore, the question arises as to whether the arrangement of the equivalent to the bacterial ε subunit in the yeast and bovine F_1F_o

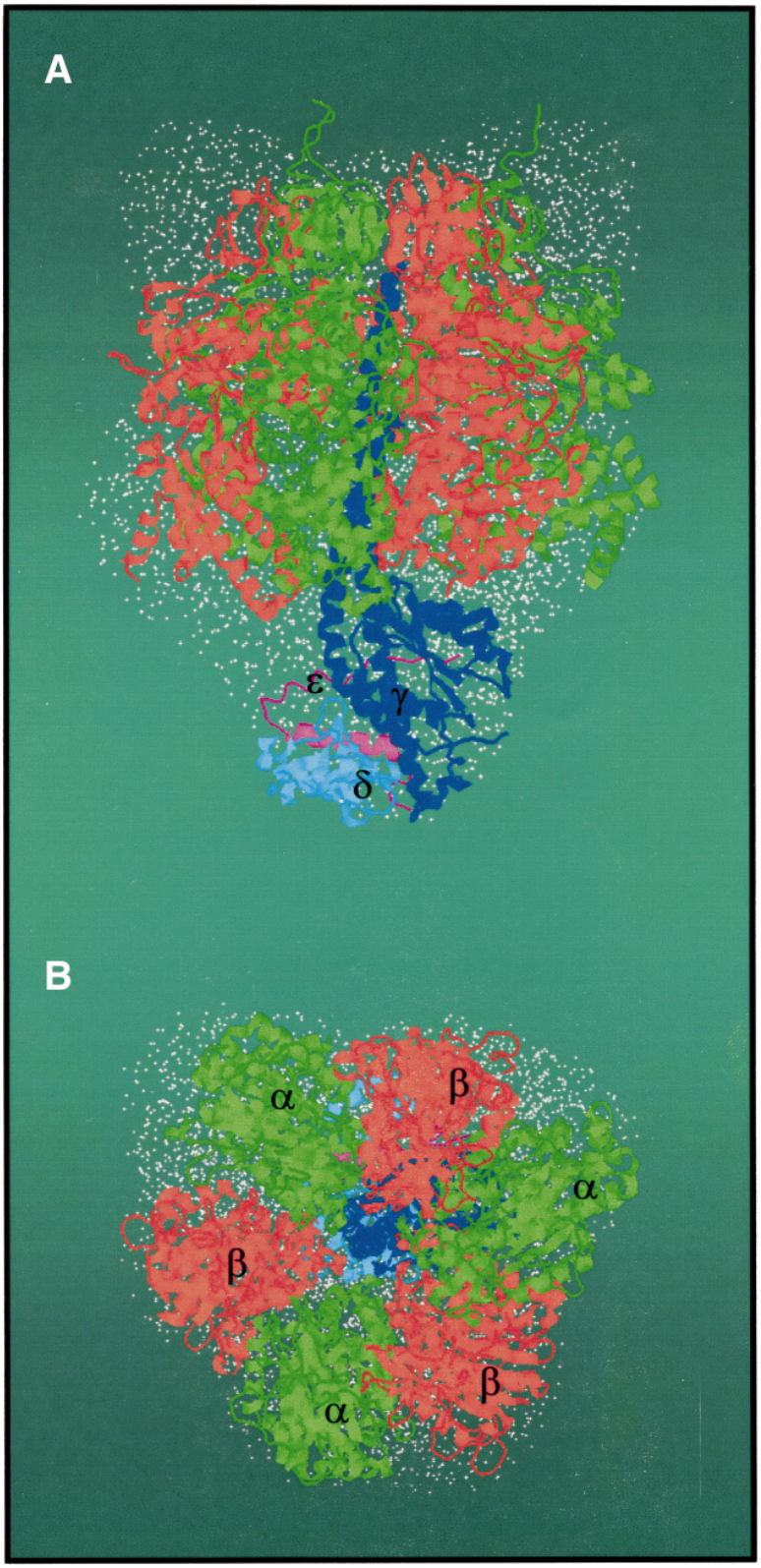

Fig. 1. The crystal structure of the bovine F_1-ATPase (Gibbons et al., 2000) superimposed on an envelope of the hydrated *E. coli* F_1-ATPase ($\alpha_3\beta_3\gamma\delta\varepsilon$), derived from X-ray small-angle scattering (shown in grey; Svergun et al., 1998b). The crystallographic cordinates were taken from the Brookhaven Protein Data Bank (Bernstein et al., 1977), entry 1E79. View A was rotated counterclockwise by 90 ° around the *y* axis and view B around the *z*-axis.

complexes reflects a trapped state during its nucleotide-dependent movement.

A model-independent approach, based upon the multipole expansion method using spherical harmonics (Stuhrmann, 1970), has been developed to complement crystallographic studies of the quaternary structure of macromolecules such as the F_1-ATPase from *E. coli* from solution X-ray scattering data. Application of this approach has led to a low-resolution (32 Å) structure of the F_1 complex under nearly physiological and saturating nucleotide conditions (Svergun et al., 1998a; Svergun et al., 1998b). The hydrated F_1-ATPase (Fig. 1, Fig. 5) is a compact molecule with a headpiece of approximately 108 Å from top to bottom and 110 Å wide. However, the overall structure is asymmetric due to the stem (stalk) that is approximately 42 Å in length and 53 Å in cross section (Svergun et al., 1998b; Grüber, 2000). These dimensions are consistent with recent data regarding the central stalk in the 2.4 Å resolution structure of the bovine F_1-ATPase ($\alpha_3\beta_3\gamma\delta_m\varepsilon_m$) with a length of 47 Å and 51 Å × 41 Å in cross section (Gibbons et al., 2000), showing the regions of the γ, δ_m and ε_m subunits are exposed at the foot of the stalk, and thereby in close contact with F_o subunits, which will consequently facilitate the mechanistic linkage of ATP hydrolysis to ion pumping (Fig. 1).

Structure and mechanism of the V_1-ATPase

Structural aspects of the V_1 complex

The idea that molecules now known to be V-ATPases may structurally resemble F-ATPases was suggested by early micrographs of insect plasma membranes (Gupta and Berridge, 1966; Anderson and Harvey, 1966), which showed repeating, spike-like units supporting globular structures. The spike-with-globule structures are widely distributed on transporting plasma membranes and were designated ‘portasomes’ (Harvey et al., 1981). Meanwhile, negatively stained membranes from bovine chromaffin granules (Schmidt et al., 1982) and the vacuolar membranes of *Neurospora crassa* (Bowman et al., 1989) were shown to contain similar structures, and sequencing of the genomic DNAs encoding V-ATPase subunits (Bowman et al., 1988) demonstrated beyond doubt that the particles are V_1-ATPases. The regulatory mechanism of reversible disassembly of the V_1 and V_o complex, first shown in the *Manduca sexta* midgut (Sumner et al., 1995) and also later in yeast (Kane, 1995), suggested that a study of the dissociated V_1 complex could provide valuable information about the structural features of this enzyme. The recovery of disassembled V_1 particles from the cytoplasm in high yield and purity (Gräf et al., 1996) made the structural description possible.

Two major advances have been made toward elucidating the quaternary structure of V_1 during the past two years. First, the gross structure of the *M. sexta* midgut V_1-ATPase was investigated by SAXS (Svergun et al., 1998b). The enzyme is highly elongated with a maximal length of about 220 Å. The solution scattering data define a hydrated complex with a headpiece approximately 145 Å in diameter and a stalk approximately 110 Å in length (Fig. 5). Second, image processing of electron micrographs of negatively stained V-ATPases from *Clostridium fervidus* (Boekema et al., 1998) and V_1-ATPase from *M. sexta* (Radermacher et al., 1999) yielded two-dimensional structures at a resolution of 18 Å and 24 Å, respectively. A comparison of the independently identified structures (Boekema et al., 1998; Svergun et al., 1998b; Radermacher et al., 1999) revealed that the headpiece consists of a pseudo-hexagonal arrangement of six masses, surrounding a seventh mass. These six masses, which are assumed to consist of the major subunits A and B, are arranged in an alternating manner (Boekema et al., 1998; Svergun et al., 1998b). The first three-dimensional reconstruction of the V_1 complex was determined at 32 Å resolution from negatively stained preparations of the *M. sexta* V_1-ATPase (Fig. 2) (Grüber et al., 2000a). A striking feature of the reconstruction is the presence of six elongated lobes, approximately 20 Å in diameter and 90 Å in length, which are parallel to the threefold axis (Fig. 2B). These lobes, which represent the alternating three copies each of subunits A and B, can be traced for most of the length of the V_1-ATPase. The hexagonal barrel of subunits A and B encloses a core of approximately 40 Å. In this model the V_1 complex is barrel-shaped, being approximately 110 Å high and 135 Å wide. At both ends of the hexagonal barrel extensions can be observed. The extensions on one side (Fig. 2A) are consistent with published two-dimensional average images of the V_1V_o-ATPase from bovine brain clathrin-coated vesicles, where elongated features (Fig. 2F–H; as, ce) can be seen at the very top of the V_1 domain (Wilkens et al., 1999). The extensions on the opposite side can be attributed to traces of the stalk, e.g. the extension visible in Fig. 2B,C. The correspondence of dimensions of the hexagonal domain as determined by SAXS (see above) and electron microscopy indicate that the stalk is not completely resolved in the three-dimensional reconstruction, presumably due to absorption and drying of the V_1 particle on the carbon film. However, a striking fact is that the shape and interdigitation of the A_3B_3 subunits, located around the periphery of the barrel, are in agreement with the three-dimensional model of the related F_1-ATPase, derived from two- (Capaldi et al., 1992; Gogol, 1994) and three-dimensional crystals of this complex (Abrahams et al., 1994; Bianchet et al., 1998; Hausrath et al., 1999), in which the alternating subunits α and β interdigitate for the full length surrounding the γ subunit.

Topology and conformational rearrangements of the V_1-ATPase

Further insights into the topology of the V_1-ATPase from *M. sexta* were obtained by tryptic digestion (Grüber et al., 2000a). Proteolytic digestion revealed that the nucleotide-binding subunit B was cleaved rapidly, yielding two fragments with apparent molecular masses of 25 and 34 kDa, whereas trypsin had no obvious effect on the major catalytic subunit A. Among the stalk subunits, C–H, subunit D was cleaved most rapidly by trypsin, followed by subunits F, G, C and H, with subunit

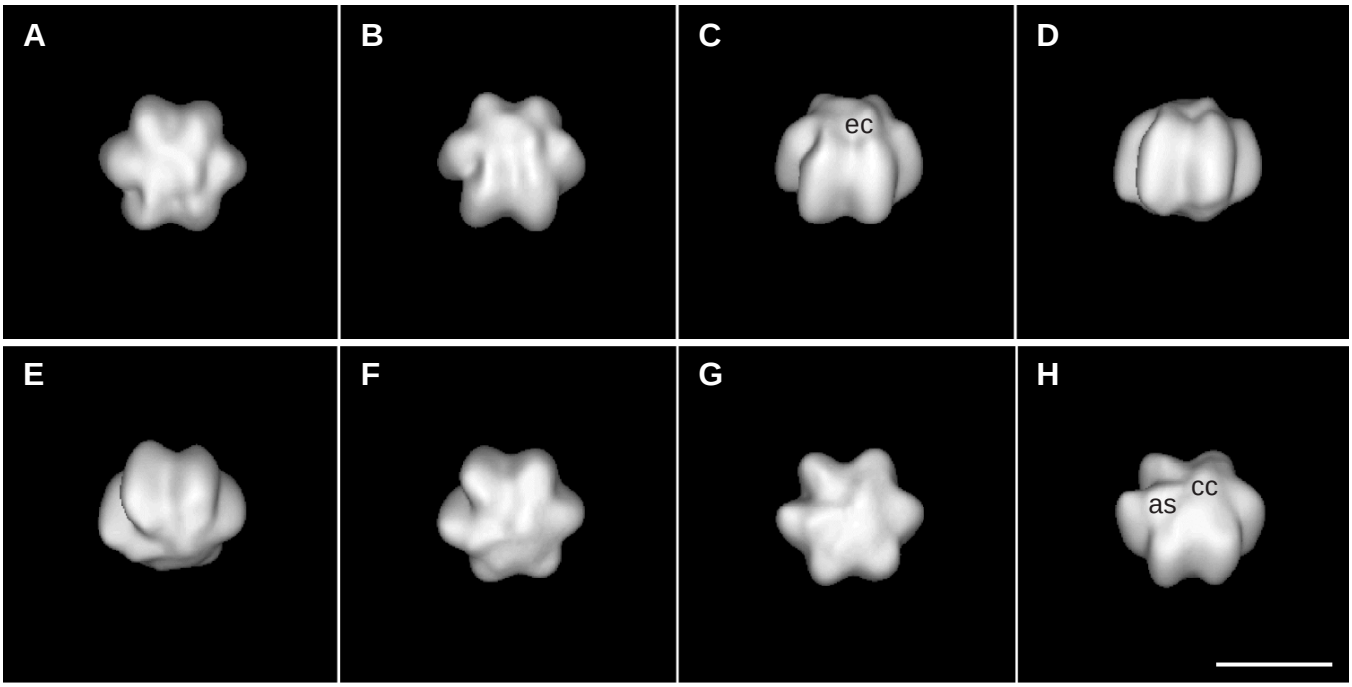

Fig. 2. Surface representation of the three-dimensional reconstruction of the V_1-ATPase from *Manduca sexta* determined from negatively stained specimens (Grüber et al., 2000a). An asymmetric (as), and a more centrally located (ce) extension can be seen above a subunit AB-interface. ec, protuberance. Bar, 100 Å.

E being modified most slowly. The rapid and slow cleavage of subunits D and E, respectively, is an important finding since both have been proposed as structural and functional homologues of the γ subunit of F-ATPases (Bowman et al., 1995; Nelson et al., 1995; Xu and Forgac, 2000). The observation that the D subunit is cleaved immediately into small peptides by trypsin is surprising; it implies that this polypeptide is exposed in the enzyme and does not support its putative role as a γ homologue (Grüber et al., 2000a).

Copper chloride-mediated disulfide formation yielded further insight into the proximity of the *M. sexta* V_1 subunits to each other and into their functional relationships. When the enzyme was incubated with 2 mmol l^{-1} CaADP on ice before Cu^{2+} treatment, two bands with apparent molecular masses of 120 and 110 kDa, consisting of the subunits A,E,F and B,H, respectively, were obtained. A B,H product did not occur when cross-linking was conducted in 2 mmol l^{-1} CaATP on ice to slow down ATP hydrolysis, implying that subunit H moves away from B to the A,B interface (Fig. 3). This interpretation is consistent with the model of the yeast V_1-ATPase, in which subunit H was located at an interface of the nucleotide-binding subunits A and B (Tomashek et al., 1997). Moreover, in the presence of CaATP, two new bands with apparent molecular masses of 42 and 44 kDa, and composed of the subunits E,G and E,F, respectively, were observed. A homologous cross-linked product consisting of subunits E and G was also been generated using dimethyl sulfoxide (Thomashek et al., 1997) and disuccinimidyl glutarate (Xu et al., 1999) as cross-linking reagents.

Taken together, the trypsin cleavage and the cross-linking data imply that one region of subunit E is shielded by the smaller subunits F and G (Fig. 3). In addition, the disulfide bonding of the catalytic A subunits with subunit E in the presence of CaADP indicates that these subunits are near neighbors. The close proximity of subunit E to subunits A, F and G would allow stalk subunit E to couple events in catalytic subunit A via stalk subunits F and G (Grüber et al., 2000a) in the V_1 portion of the V_1V_o-ATPase to events in the ion-translocating V_o portion (Fig. 3; Tomashek et al., 1997).

Redox modulation as a regulation of V-ATPases

There is abundant evidence that V-ATPase activity is modulated by disulfide-bond formation (Feng and Forgac, 1992; Forgac, 2000). A mechanism of reversible disulfide-bond formation between cysteine residues (Cys_{254} and Cys_{532}) of the catalytic A subunit was proposed to regulate the V-ATPase *in vivo* (Oluwatosin and Kane, 1995; Forgac, 2000). A mechanism was proposed in which disulfide bond formation is quickly followed by dissociation of the V_1 and V_o complexes (Dschida and Bowman, 1995), implying that nucleotide-binding and hydrolysis in the A subunit of the V_1 domain have to be linked by the stalk region to ion translocation in the membrane-bound V_o domain. Recently SAXS experiments showed that reducing the V_1-ATPase of *M. sexta* leads to significant changes in the overall dimensions of the complex. The radius of gyration of the oxidized and reduced enzyme are 62±6 Å and 58±6 Å, respectively, whereas the maximum dimension of both complexes remains constant at 220±10 Å (Grüber et al., 2000b). The shapes of both complexes (Fig. 4) were determined *ab initio* at a

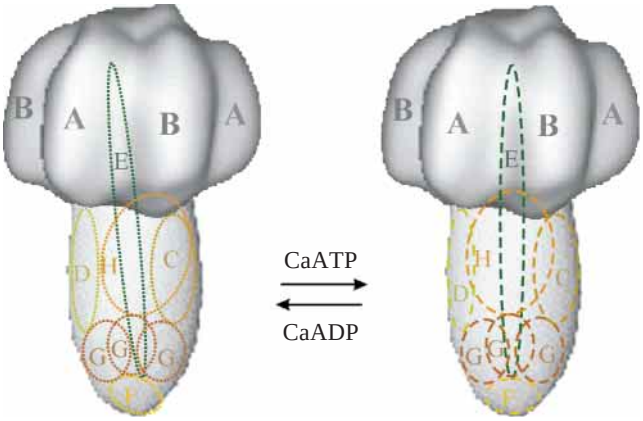

Fig. 3. Model of the subunit arrangement in the V_1-ATPase from *M. sexta* and its nucleotide-dependent rearrangement, based on the combination of the solution-scattering X-ray data, the three-dimensional reconstruction (dark grey) and biochemical studies (Grüber et al., 2000a). Subunits C–H are placed within the envelope of the stalk of V_1 from *M. sexta* as determined by SAXS data (Svergun et al., 1998b).

resolution of 27 Å by a simulated annealing procedure, based on a representation of the structure in terms of dummy atoms (Svergun, 1999). Both low-resolution structures have a characteristic mushroom-like shape with a central stalk of significant length, similar to the identified structures of the V_1-ATPase from *Clostridium fervidus* (Boekema et al., 1998) and *M. sexta* (Svergun et al., 1998), using electron microscopy and SAXS, respectively. Comparison of the oxidized and reduced models indicates that the main conformational changes upon reduction take place in both the crown-like region at the very top of the globular headpiece, where the major subunits A and B are located, and in the elongated stalk. Both regions evolve into an arrow-like shape after reduction (Grüber et al., 2000b). Based on homology of

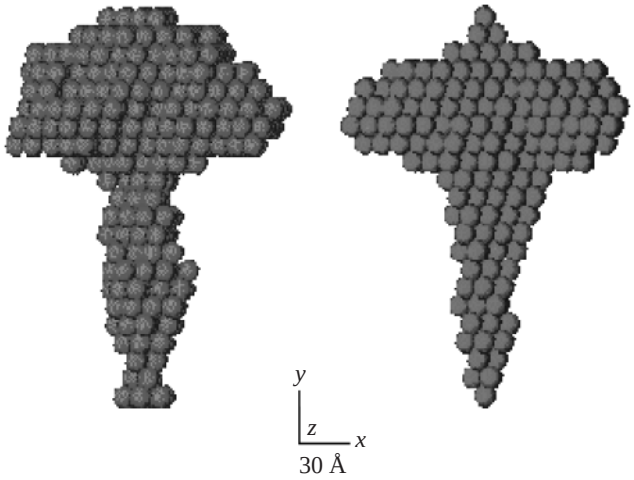

Fig. 4. Low-resolution models of the oxidized (left) and reduced V_1-ATPase (right) from *M. sexta* (Grüber et al., 2000b).

the subunits A and B to the related F-ATPase subunits β and α, respectively (Nelson, 1992), whose N termini form a β-barrel domain in a crown-like fashion (Bakhtiari et al., 1999), the conformational changes at the top of the V_1-ATPase are presumably due to rearrangements in the N termini of the A and B subunits. As shown more recently by three-dimensional reconstructions of the related F_1F_o-ATPase from *E. coli*, a crown-like shape, which is missing in the absence of the nucleotide (Böttcher et al., 2000), evolves upon binding of the non-cleavable nucleotide analogue AMP-PNP into the catalytic β subunit. The appearance of the crown has been attributed to rearrangements in the N-terminal domains of the α and β subunits, located at the very top of F_1. Moreover, when AMP-PNP or ADP are bound to the catalytic site, subunit β assumes its *closed* conformation, in which the adenine-binding pocket moves into close proximity with the phosphate-binding domain, the P-loop; it moves away when the binding-site is empty (*open* conformation), as shown by the crystallographic model of the $\alpha_3\beta_3\gamma$ subcomplex of bovine heart mitochondrial F_1-ATPase (Abrahams et al., 1994). There is a striking similarity between the crown structure of the *E. coli* F_1F_o-ATPase (Böttcher et al., 2000) that evolves after binding of AMP-PNP (*closed* conformation) and the crown-like feature that is observed in the oxidized V_1-ATPase (Grüber et al., 2000b). In this state, the catalytic A subunit is proposed to be in a *closed* conformation (Forgac, 2000), and alters into a wedge-like shape after reduction of V_1. In summary, the structural changes in the headpiece, upon reduction of the enzyme, correspond with alterations of the protuberance of the stalk into a wedge-like feature, which enables the enzyme to transmit the activating movements that take place in the V_1 headpiece to the V_o complex.

The archaeal A_1-ATPase

Like F_1 and V_1 complexes of F- and V-ATPases, the A_1 complex of archaeal ATPases possesses a pseudo-hexagonal arrangement of the major subunits A and B, as proposed from two-dimensional images of the thermoacidophilic archaea *Sulfolobus acidocaldarius* and *Methanosarcina mazei* Gö1 (Lübben et al., 1988; Wilms et al., 1996). However, in contrast to the related F_1- and V_1-ATPases described above, little is known about the overall structure of the enzyme. This information gap is largely due to the instability of the isolated complexes (Wilms et al., 1996; V. Müller, unpublished). A new avenue of research was opened by the cloning and sequencing of the A_1A_o-ATPase encoding genes from methanogenic archaea. In *M. mazei* Gö1, the genes encoding the ATPase are clustered on the chromosome and comprise an operon. A fragment containing *ahaE*, *ahaC*, *ahaF*, *ahaB*, *ahaA* and *ahaG* was cloned in an overexpression vector and transformed into the F_1F_o-ATPase negative mutant *E. coli* DK8, which produced an A_1-ATPase upon induction of gene expression. This A_1 complex is made up of the five different subunits A, B, C, D and F, with apparent molecular masses of 64, 51, 41, 24 and 11 kDa, respectively, as estimated from the

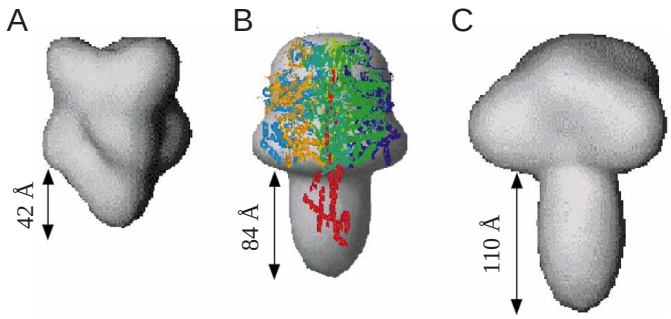

Fig. 5. Comparison of the low-resolution envelopes (shown in grey) of *E. coli* F_1- (A), *M. mazei* Gö1 A_1- (B) and *M. sexta* V_1-ATPase (C) (Grüber et al., 2001). In the structure of the $\alpha_3\beta_3\gamma$ subcomplex of related *E. coli* F_1-ATPase (entry 1D8D) is superimposed on the envelope A_3B_3CDF complex of the A_1-ATPase from *M. mazei* (Grüber et al., 2001).

amino acid sequences (Wilms et al., 1996); subunit E was not produced in *E. coli* (T. Lemker and V. Müller, unpublished). Based on SAXS data, the A_3B_3CDF-complex (Fig. 5) comprises a headpiece approximately 94 Å long and 92 Å wide (Grüber et al., 2001). Superposition of the low-resolution structure of the A_1 complex with the atomic model of the $\alpha_3\beta_3\gamma$ complex of the related F_1-ATPase from *E. coli* (Hausrath et al., 1999) reveals a striking similarity, especially with respect to the disposition of the nucleotide binding subunits α and β, the homologs of subunits B and A, respectively (Fig. 5B; Grüber et al., 2001). This structural similarity lends support to the view that A- and F-ATPases share a common catalytic mechanism for ATP synthesis. The overall structure of the hydrated particle is asymmetric because of the stalk, which is approximately 84 Å long and 60 Å in diameter. The shape and length of the stalk strongly resemble those in the stalk domain of the related V_1-ATPase from *M. sexta* (see Fig. 5) (Svergun et al., 1998b; Grüber et al., 2000b). A comparison of the overall structures of the A_1- and V_1-ATPases (Svergun et al., 1998b; Grüber et al., 2001) with the low resolution (Svergun et al., 1998a; Svergun et al., 1998b) and atomic models of the *E. coli* (see Fig. 5; Hausrath et al., 1999) and bovine heart F_1-ATPase (Gibbons et al., 2000) identified major differences between these molecules. In particular, the F_1-ATPase differs in shape from the other two enzymes and has a significantly shorter stalk, being approximately 40–45 Å long and 50–53 Å wide (Gibbons et al., 2000; Grüber, 2000). These differences are consistent with the proposed evolutionary linkage of A_1- and V_1-ATPases, which are thought to have evolved from common ancestral genes (Iwabe et al., 1989; Ihara et al., 1992). Tryptic digestion studies of the A_3B_3CDF complex have shown that the subunits C and F are exposed in the complex, whereas subunit D is well protected from the effect of trypsin (Grüber et al., 2001). The shielding of subunit D from trypsin is an important finding since this subunit has been proposed as the structural and functional homolog of the γ subunit of F-ATPases (Müller et al., 1999; Grüber et al., 2001). In experiments where $CuCl_2$ was added after preincubation of MgATP, the cross-linked product A-D was formed, which was absent in the presence of MgADP+P_i (Ü. Coskun, J. Godovac-Zimmermann, T. Lemker, V. Müller and G. Grüber, unpublished data). The disulfide bond that forms between catalytic subunit A and subunit D in the presence of MgATP indicates that these subunits are near neighbors. Furthermore, the absence of an A-D product, when MgADP+P_i are bound, also indicates a rearrangement of these subunits due to nucleotide binding. Taken together, the shielding of A_1 subunit D from trypsin and the nucleotide-dependent cross-linking of A to D are reminiscent of the shielding of the V_1 subunit E from the protease and the substrate-dependent proximity of E to the catalytic A subunits (Grüber et al., 2000a), which suggests in turn that A_1 subunit D and V_1 subunit E may have similar functional roles.

Conclusions and future perspectives

Phylogenetic studies show that A- and V-ATPases evolved from a common ancestor (Iwabe et al., 1989; Ihara et al., 1992). The evolutionary relationship of both enzymes, and their relationship to F-ATP synthases, were confirmed by comparing the low-resolution structure of the A_1- F_1- and V_1-ATPases, which revealed that a knob-and-stalk-like shape is common to all three complexes. The stalk domains of the more closely related A_1 and V_1 are remarkably similar in shape and dimensions, and are different in these respects from the F_1-ATPase. Despite the differences in structure, A_1A_o and F_1F_o enzymes function as ATP synthases in cells whereas the V_1V_o-ATPase works as an ATP-driven ion pump. The elucidation of the structural basis for this functional difference is a challenge for future studies.

Further evidence for a closer relationship between A- and V-ATPases than either has to F-ATPase is found by comparing A_o and V_o to F_o domains. Unlike the F_o domain (see above) the V_o and A_o domains contain only two membrane integral subunits, *a* (I in A_1A_o-ATPases) and *c* (the so called proteolipid). There is a surprising variation in the number of proteolipid subunits: two additional proteolipid subunits, *c′* and *c″*, both of which have homology to subunit *c* (Stevens and Forgac, 1997) are found in some V-ATPases, the F-ATPase from the bacterium *Acetobacterium woodii* contains two 8-kDa proteolipid subunits, c_2 and c_3, and the A-ATPase from the archaeon *Archeoglobus fulgidus* contains two 8 kDa proteolipids (Müller et al., 1999; Müller et al., 2001). Moreover, there is an astonishing variability in the size of the proteolipids in archaeal A-ATPases with two, four or six transmembrane helices and a variable number of conserved ionizable groups per monomer (Müller et al., 1999). A proteolipid with four transmembrane helices but only one ionizable group has recently been described in the bacterial F_1F_o-ATPase from *A. woodii* (Aufurth et al., 2000). Regarding these remarkably complex machines there still remains the question of how the energy coupling between the proposed ion-gradient-driven motion within the A_o and V_o domains is coupled by their stalks to the reversal of the ATP-driven motion in A_1 and V_1 domains.

This research was supported by grants from the Deutsche Forschungsgemeinschaft to V.M. (Mu801/10), H.W. (Wi 698 and SFB 431) and G.G. (GR 1475/6-1), respectively, and from the National Institutes of Health to W.R.H. (AI 22444).

References

Abrahams, J. P., Leslie, A. G. W., Lutter, R. and Walker, J. E. (1994). Structure at 2.8 Å resolution of F_1-ATPase from bovine heart mitochondria. *Nature* **370**, 621–628.

Anderson, E. and Harvey, W. R. (1966). Active transport by the Cecropia midgut II. Fine structure of the midgut epithelium. *J. Cell Biol*. **31**, 107–134.

Aufurth, S., Schägger, H. and Müller, V. (2000). Identification of subunits *a*, *b*, and c_1 from *Acetobacterium woodii* Na^+-F_1F_o-ATPase: subunits c_1, c_2, and c_3 constitute a mixed oligomer. *J. Biol. Chem*. **275**, 33297–33301.

Bakhtiari, N., Lai-Zhang, J., Yao, B. and Mueller, D. M. (1999). Structure/Function of the β-Barrel Domain of F_1-ATPases in the Yeast *Saccharomyces cereviisiae*. *J. Biol. Chem*. **265**, 960–966.

Bernstein, F. C., Koetzle, T. F., Williams, G. J. B., Meyer, E. G., Jr., Brice, M. D., Rodgers, J. R., Kennard, O., Shimanouchi, T. and Tasumi, M. (1977). The Protein Data Bank: a computer-based archival file for macromolecular structures. *J. Mol. Biol*. **112**, 535–542.

Bianchet, M. A, Hullihen, J. Pedersen, P. L. and Amzel, M. L. (1998). The 2.8 Å structure of rat liver F_1-ATPase: Configuration of a critical intermediate in ATP synthesis/hydrolysis. *Proc. Natl. Acad. Sci. USA* **95**, 11065–11070.

Boekema, E. J., Ubbink-Kok, T., Lolkema, J. S., Brisson, A. and Konings, W. N. (1998). Structure of V-type-ATPase from *Clostridium fervidus* by electron microscopy. *Photosyn. Res.* **57**, 267–273.

Böttcher, B. and Gräber, P. (2000). The structure of the H^+-ATP synthase from chloroplasts and its subcomplexes as revealed by electron microscopy. *Biochim. Biophys. Acta* **1458**, 404–416.

Böttcher, B., Schwarz, L. and Gräber, P. (2000). Direct visualization of conformational changes in EF(0)F(1) by electron microscopy. *J. Mol. Biol*. **281**, 757–762.

Bowman, E. J., Tenny, K. and Bowman, B. J. (1988). Isolation of genes encoding the *Neurospora* vacuolar ATPase. Analysis of *vma-1* encoding the 67 kDa subunit reveals homology to other ATPases. *J. Biol. Chem.* **263**, 13994–14001.

Bowman, B. J., Dschida, W. J., Harris, T. and Bowman, E. J. (1989). The vacuolar ATPase of *Neurospora crassa* contains an F_1–like structure. *J. Biol. Chem*. **264**, 15606–15612.

Bowman, E. J., Steinhardt, A. and Bowman, B. J. (1995). Isolation of the *vma-4* gene encoding the 26 kDa subunit of the *Neurospora crassa* vacuolar ATPase. *Biochim. Biophys. Acta* **1237**, 95–98.

Capaldi, R. A., Aggeler, R., Gogol, E. P. and Wilkens, S. (1992). Structure of the *Escherichia coli* ATP synthase and role of the γ and ε subunits in coupling catalytic site and proton channeling functions. *J. Bioenerg. Biomembr*. **24**, 435–439.

Capaldi, R. A., Aggeler, R., Wilkens, S. and Grüber, G. (1996). Structural changes in the γ and ε subunits of the *Escherichia coli* F_1F_o-type ATPase during energy coupling. *J. Bioenerg. Biomembr*. **28**, 397–401.

Dimroth, P. (1997). Primary sodium ion translocating enzymes. *Biochim. Biophys. Acta* **1318**, 11–51.

Dschida, W. J. and Bowman, B. J. (1995). The vacuolar ATPase: sulfite stabilization and the mechanism of nitrate inactivation. *J. Biol. Chem.* **270**, 1557–1563.

Feng, Y. and Forgac, M. (1992). A novel mechanism for regulation of vacuolar acidification. *J. Biol. Chem.* **267**, 19769–19772.

Fillingame, R. H. (1996). Membrane sectors of F- and V-type H^+-transporting ATPases. *Curr. Opin. Struct. Biol.* **6**, 491–498.

Forgac, M. (2000). Structure, mechanism and regulation of the clathrin-coated vesicle and yeast vacuolar H^+-ATPases. *J. Exp. Biol.* **203**, 71–80.

Gibbons, C., Montgomery, M. G., Leslie, A. G. W. and Walker, J. E. (2000). The structure of the central stalk in bovine F_1-ATPase at 2.4 Å resolution. *Nat. Struct. Biol.* **7**, 1055–1061.

Giraud, M.-F. and Velours, J. (1994). ATP synthase of yeast mitochondria. Isolation of the F_1 δ subunit, sequence and disruption of the structural gene. *Eur. J. Biochem.* **222**, 851–859.

Gogol, E. P., Aggeler, R., Sagermann, M. and Capaldi, R. A. (1989). Cryoelectron microscopy of *Escherichia coli* F_1 adenosintriphosphatase decorated with monoclonal antibodies to individual subunits of the complex. *Biochemistry* **28**, 4717–4724.

Gogol, E. P. (1994). Electron microscopy of the F_1F_o-ATP synthase – from structure to function. *Microsc. Res. Tech.* **27**, 294–306.

Gräf, R., Harvey, W. R. and Wieczorek, H. (1996). Purification and properties of a cytosolic V_1-ATPase. *J. Biol. Chem.* **271**, 20908–20913.

Groth, G. and Pohl, E. (2001). The structure of the chloroplast F_1-ATPase at 3.2 Å resolution. *J. Biol. Chem.* **276**, 1345–1352.

Grüber, G. and Capaldi, R. A. (1996). The trapping of different conformations of the *Escherichia coli* F_1-ATPase by disulfide bond formation: Effect on nucleotide binding affinities on the catalytic sites. *J. Biol. Chem.* **271**, 32623–32628.

Grüber, G., Hausrath, A., Sagermann, M. and Capaldi, R. A. (1997). An improved purification of ECF_1 and ECF_1F_o by using a cytochrome bo-deficient strain of *Escherichia coli* facilitates crystallization of these complexes. *FEBS Lett.* **410**, 165–168.

Grüber, G. (2000). Structural and functional features of the *Escherichia coli* F_1-ATPase. *J. Bioenerg. Biomembr.* **32**, 341–346.

Grüber, G., Radermacher, M., Ruiz, T., Godovac-Zimmermann, J., Canas, B., Kleine-Kohlbrecher, D., Huss, M., Harvey, W. R. and Wieczorek, H. (2000a). Three-dimensional structure and subunit topology of the V_1-ATPase from *Manduca sexta* midgut. *Biochemistry* **39**, 8609–8616.

Grüber, G., Svergun, D. I., Godovac-Zimmermann, J., Harvey, W. R., Wieczorek, H. and Koch, M. H. J. (2000b). Evidence for major structural changes in the *Manduca sexta* midgut V_1-ATPase due to redox-modulation: A small-angle X-ray scattering study. *J. Biol. Chem.* **275**, 30082–30087.

Grüber, G., Svergun, D. I., Coskun, Ü., Lemker, T., Koch, M. H. J., Schägger, H. and Müller, V. (2001). Structural insights into the A_1-ATPase from the archaeon, *Methanosarcina mazei* Gö1. *Biochemistry* **40**, 1890–1896.

Gupta, B.L. and Beridge, M. L. (1966). A coat of repeating subunits on the cytoplasmic surface of the plasma membrane in the rectal papillae of the blowfly, *Calliphora erythrocephala* (Meig.), studied *in situ* by electron microscopy. *J. Cell Biol*. **29**, 376–382.

Harvey, W. R., Cioffi, M. and Wolfersberger, M. G. (1981). Portasomes as coupling factors in active ion transport and oxidative phosphorylation. *Amer. Zool*. **21**, 775–791.

Hausrath, A. C., Grüber, G., Matthews, B. W. and Capaldi, R. A. (1999). Structural features of the γ subunit of the *Escherichia coli* F_1-ATPase revealed by a 4.4 Å resolution map obtained by X-ray crystallography. *Proc. Natl. Acad. Sci. USA* **96**, 13697–13702.

Ihara, K., Abe, T., Sugimura, K.-I. and Mukohata, Y. (1992). Halobacterial A-ATP synthase in regulation to V-ATPase. *J. Exp. Biol.* **172**, 475–485.

Iwabe, N., Kuma, K.-I., Hasegawa, M., Osawa, S. and Miyata, T. (1989). Evolutionary relationship of archaebacteria, eubacteria, and eukaryotes inferred from phylogenetic trees of duplicated genes. *Proc. Natl. Acad. Sci. USA* **86**, 9355–9359.

Junge, W., Lill, H. and Engelbrecht, S. (1997). ATP synthase: an electrochemical transducer with rotary mechanics. *Trends Biochem. Sci.* **22**, 420–423.

Kane, P. M. (1995). Disassembly and reassembly of the yeast vacuolar H^+-ATPase *in vivo*. *J. Biol. Chem.* **270**, 17025–17032.

Leslie, A. G. W. and J. E. Walker (2000). Structural model of the F_1-ATPase and the implications for rotary catalysis. *Phil. Trans. R. Soc. Lond. B* **355**, 465–472.

Lübben, M., Lünsdorf, H. and Schäfer, G. (1988). Archaebacterial ATPase: studies on subunit composition and quaternary structure of the F_1-analogous ATPase from *Sulfolobus acidocaldarius*. *Biol. Chem. Hoppe-Seyler* **369**, 1259–1266.

Masaike, T., Mitome, N., Noji, H., Muneyuki, E., Yasuda, R., Kinosita, K., Jr. and Joshida, M. (2000). Rotation of F_1-ATPase and the hinge residues of the β subunit. *J. Exp. Biol.* **203**, 1–8.

Mendel-Hartvig, J. and Capaldi, R. A. (1991). Nucleotide-dependent and dicyclohexylcarbodiimide-sensitive conformational changes in the ε subunit of *Escherichia coli* ATP synthase. *Biochemistry* **30**, 10987–10991.

Mitchell, P. (1961). Coupling of phosphorylation to electron and hydrogen transfer by a chemiosmotic type of mechanism. *Nature* **191**, 144–148.

Müller, V., Ruppert, C. and Lemker, T. (1999). Structure and function of the A_1A_o-ATPases from Methanogenic Archaea. *J. Bioenerg. Biomembr.* **31**, 15–28.

Müller, V., Aufurth, S. and Rahlfs, S. (2001). The Na^+ cycle in *Acetobacterium woodii*: identification and characterization of the Na^+

translocating F_1F_o-ATPase with a mixed oligomer of 8 and 16 kDa proteolipids. *Biochim. Biophys. Acta* **1505**, 108–120.

Nelson, N. (1992). Evolution of organellar proton-ATPases. *Biochim. Biophys. Acta* **1100**, 109–124.

Nelson, H., Mandiyan, S. and Nelson, N. (1995). A bovine cDNA and a yeast gene (VMA8) encoding the subunit D of the vacuolar H^+-ATPase. *Proc. Natl. Acad. Sci. USA* **92**, 497–501.

Oluwatosin, Y. E. and Kane, P. M. (1995). Mutations in the CYS4 gene provide evidence for regulation of the yeast V-ATPase by oxidation and reduction in vivo. *J. Biol. Chem.* **272**, 28149–28157.

Pänke, O., Gumbiowsky, K., Junge, W. and Engelbrecht, S. (2000). F-ATPase: specific observation of the rotating c subunit oligomer of EF_oEF_1. *FEBS Lett.* **472**, 34–38.

Pedersen, P. L., Young, H. K. and Sangjin, H. (2000). ATP synthases in the Year 2000: Evolving views about the structures of these remarkable enzyme complexes. *J. Bioenerg. Biomembr.* **32**, 325–332.

Radermacher, M., Ruiz, T., Harvey, W. R., Wieczorek, H. and Grüber, G. (1999). Molecular architecture of *Manduca sexta* midgut V_1-ATPase visualized by electron microscopy. *FEBS Lett.* **453**, 383–386.

Rastogi, V. K. and Girvin, M. E. (1999). Structural changes linked to proton translocation by subunit c of the ATP synthase. *Nature* **402**, 263–268.

Rodgers, A. J. W. and Wilce, M. C. J. (2000). Structure of the γ/ε complex ATP synthase. *Nat. Struct. Biol.* **7**, 1051–1054.

Sambongi, Y., Iko, Y., Tanabe, M., Omote, H., Iwamoto-Kihara, A., Ueda, I., Yanagida, T., Wada, Y. and Futai, M. (1999). Mechanical rotation of the c subunit oligomer in ATP synthase (F_oF_1): direct observation. *Science* **286**, 1722–1724.

Schäfer, G., Engelhard, M. and Müller, V. (1999). Bioenergetics of the Archaea. *Microbiol. Mol. Biol. Rev.* **63**, 570–620.

Schmidt, W., Winkler, H. and Plattner, H. (1982). Adrenal chromaffin granules: evidence for an ultrastructural equivalent of the proton pumping ATPase. *Eur. J. Cell Biol.* **27**, 96–104.

Seelert, H., Poetsch, A., Dencher, N. A., Engel, A., Stahlberg, H. and Müller, D. J. (2000). Proton-powered turbine of a plant motor. *Nature* **405**, 418–419.

Shirakihara, Y., Leslie, A. G. W., Abrahams, J. P., Walker, J. E., Ueda, T., Sekimoto, Y., Kambara, M., Saika, K., Kagawa, Y. and Yoshida, M. (1997). The crystal structure of the nucleotide-free $\alpha_3\beta_3$ subcomplex of F1-ATPase from the thermophilic Bacillus PS3 is a symmetric trimer. *Structure* **5**, 825–836.

Stahlberg, H., Müller, D. J., Suda, K., Fotiadis, D., Engel, A., Meier, T., Matthey, U. and Dimroth, P. (2001). Bacterial Na^+-ATP synthase has an undecameric rotor. *EMBO Rep.* **2**, 229–233.

Stevens, T. H., and Forgac, M. (1997). Structure, function and regulation of the vacuolar H^+-ATPase. *Ann. Rev. Cell Dev. Biol.* **13**, 779–808.

Stock, D., Leslie, A. G. W. and Walker, J. E. (1999). Molecular architecture of the rotary motor in ATP synthase. *Science* **286**, 1700–1705.

Stuhrmann, H. B. (1970). Interpretation of small-angle scattering functions of dilute solutions and gases. A representation of the structures related to a one-particle-scattering function. *Acta Crystallogr. A* **26**, 297–306.

Sumner, J. P., Dow, J. A. T., Earley, F. G., Klein, U., Jäger, D. and Wieczorek, H. (1995). Regulation of plasma membrane V-ATPase activity by dissociation of peripheral subunits. *J. Biol. Chem.* **270**, 5649–5653.

Svergun, D. I., Aldag, I., Sieck, T., Altendorf, K., Koch, M. H. J., Kane, D. J., Kozin, M. B. and Grüber, G. (1998a). A model of the quaternary structure of the *Escherichia coli* F_1-ATPase from X-ray solution scattering and evidence for structural changes in the δ subunit during ATP hydrolysis. *Biophys. J.* **75**, 2212–2219.

Svergun, D. I., Konrad, S., Huss, M., Koch, M. H. J., Wieczorek, H., Altendorf, K., Volkov, V. V. and Grüber, G. (1998b). Quaternary structure of V_1 and F_1 ATPase: Significance of structural homologies and diversities. *Biochemistry* **37**, 17659–17663.

Svergun, D. I. (1999). Restoring low resolution structure of biological macromolecules from solution scattering using simulated annealing. *Biophys. J.* **76**, 2879–2886.

Tomashek, J. J., Graham, L. A., Hutchins, M. U., Stevens, T. H. and Klionsky, D. J. (1997). V_1-situated stalk subunits of the yeast vacuolar proton-translocating ATPase. *J. Biol. Chem.* **272**, 26787–26793.

Tsunoda, S., Aggeler, R., Yoshida, M. and Capaldi, R. A. (2001). Rotation of the c subunit oligomer in fully functional F_1F_o-ATP synthase. *Proc. Natl. Acad. Sci. USA* **98**, 898–902.

Uhlin, U., Cox, G. B. and Guss, J. M. (1997). Crystal structure of the ε subunit of the proton-translocating ATP synthase from *Escherichia coli*. *Structure* **5**, 1219–1230.

Watts, S. D., Zhang, Y., Fillingame, R. H. and Capaldi, R. A. (1995). The γ subunit in the *Escherichia coli* ATP synthase complex (ECF_1F_o) extends through the stalk and contacts the c subunits of the F_o part. *FEBS Lett.* **368**, 235–238.

Watts, S. D, T**ang, C. and Capaldi, R. A.** (1996). The stalk region of the *Escherichia coli* ATP synthase. Tyrosine 205 of the γ subunit is in the interface between the F_1 and F_o parts and can interact with both the ε and c oligomer. *J. Biol. Chem.* **271**, 28341–28347.

Wieczorek, H., Brown, D., Grinstein, S., Ehrenfeld, J. and Harvey, W. R. (1999). Animal plasma membrane energization by proton-motive V-ATPases. *BioEssays* **21**, 637–648.

Wieczorek, H., Grüber, G., Harvey, W. R., Huss, M., Merzendorfer, H. and Zeiske, W. (2000). Structure and regulation of insect plasma membrane H^+ V-ATPase. *J. Exp. Biol.* **203**, 127–135.

Wilkens, S., Dahlquist, F. W., McIntosh, L. P., Donaldson, L. W. and Capaldi, R. A. (1995). Structural features of the ε subunit of the *Escherichia coli* ATP synthase determined by NMR spectroscopy. *Nature Struct. Biol.* **2**, 961–967.

Wilkens, S., Dunn, S. D., Chandler, J., Dahlquist, F. W. and Capaldi, R. A. (1997). Solution structure of the N-terminal domain of the δ subunit of the *E. coli* ATP synthase. *Nature Struct. Biol.* **4**, 198–201.

Wilkens, S. and Capaldi, R. A. (1998). Solution structure of the ε subunit of the F_1-ATPase from *Escherichia coli* and interactions of this subunit with β subunits in the complex. *J. Biol. Chem.* **273**, 26645–26651.

Wilkens, S., Vasilyeva, E. and Forgac, M. (1999). Structure of the vacuolar ATPase by electron microscopy. *J. Biol. Chem.* **274**, 31804–31810.

Wilms, R., Freiberg, C., Wegerle, E., Meier, I., Mayer, F. and Müller, V. (1996). Subunit structure and organization of the genes of the A_1A_o-ATPase from the Archaeon *Methanosarcina mazei* Gö1. *J. Biol. Chem.* **271**, 18843–18852.

Xu, T., Vasilyeva, E. and Forgac, M. (1999). Subunit interactions in the clathrin-coated vesicle vacuolar (H^+)-ATPase complex. *J. Biol. Chem.* **274**, 28909–28915.

Xu, T. and Forgac, M. (2000). Subunit D (Vma8p) of the yeast vacuolar H^+-ATPase plays a role in coupling of proton transport and ATP hydrolysis. *J. Biol. Chem.* **275**, 22075–22081.